ARTICLE

Theoretical Study of Hydrogen Bonding Interaction of 1:1 Dimer of HNO with HArF

Ying Liu[a,b*], Wen-qing Liu[a], Hai-yang Li[c], Yong Yang[a,b], Shuang Cheng[a,b]

a. Key Laboratory of Environmental Optics & Technology, Anhui Institute of Optics & Fine Mechanics, Chinese Academy of Sciences, Hefei 230031, China; b. Graduate School of Chinese Academy of Sciences, Beijing 100039, China; c. Dalian Institute of Chemical Physics, Chinese Academy of Sciences, Dalian 116023, China

The hydrogen bonding interaction of 1:1 dimer formed between HNO and HArF molecule has been completely investigated in the present study using Second-order Møller-Plesset Perturbation (MP2) method in conjunction with 6-311+G**, 6-311++G** and 6-311++G(2d,2p) basis sets. The standard and CP-corrected calculations have been employed to determine the equilibrium structures, the vibrational frequencies and interaction energies. The interaction energies of the dimers were also calculated at G2MP2 level. Two stable structures are found as the minima. Dimer I(H···F)is a five-membered cyclic hydrogen bonded structure and is more stable than the Dimer II(H···O). The blue-shifted N−H···F hydrogen bond is confirmed with standard and CP-corrected calculations by the MP2 and DFT methods in conjunction with different basis sets. The results obtained at MP2 in conjunction with different basis sets show there is a red-shifted hydrogen bond (Ar−H···O) in the Dimer II(H···O). The topological and electronic properties, the origin of red- and blue-shifted hydrogen bonds were investigated at MP2/6-311++G(2d,2p) with CP corrected calculations. From the NBO analysis, the reasonable explanations for the red- and blue-shifted hydrogen bonds were proposed.

Key words: Blue-shifted hydrogen bond, Atoms in molecules topological analysis, Natural bond orbital analysis, Electron density redistribution

I. INTRODUCTION

There have been a lot of recent scientific investigations of the properties of neutral rare-gas compounds, stimulated by the experimental discovery of HArF, the first known chemical compound of Ar [1]. The preparation of various neutral noble-gas molecules HNgY (Ng, noble gas atom; Y, electronegative atom or group) in solid noble-gas matrix has opened a fascinating new chapter in the study of noble-gas chemistry [2,3]. In particular, the recent discovery of HArF [1,4], HKrF [5], solvated HXeOH [6], noble-gas inserted hydrocarbons [7-9], and various noble-gas coordinated metal complexes [10-13] has attracted considerable new attentions to this field [14]. The bonding in these unusual molecules is mainly characterized by a H−Rg bond and an ionic Rg−F bond with the complex exhibiting $(HRg)^+F^-$ ion-pair character [15,16]. It has been shown that these molecules are very polar with large dipole moments (e.g., $\sim$7D for HArF) [1,15,17]. Thus these molecules are expected to form dipole or hydrogen-bond complexes with small molecules. Recently, complexations of HArF, HKrF and HKrCl with N_2, P_2 and CO, have been theoretically predicted or experimentally studied [18-22]. Significant blue-shifts

of the H−Ng stretching frequencies were observed in most cases while for HArF···P_2 a large red shift was predicted [21]. So far most of the hydrogen-bonded complexes that have been studied are HArF and other molecules. To our knowledge, the investigations on the interactions between HArF and the radicals are scarce. Because radicals are not stable species, the experimental studies on molecules and radicals hydrogen bonds are fairly difficult to be conducted. Not much useful information can be obtained from the experimental studies for the structures and energies of hydrogen-bonded complexes formed by the molecules and radicals, either. However, theoretical studies can provide more information about hydrogen-bonded complexes formed by the molecules and radicals and are expected to be important.

HNO is important in the processes such as pollution formation, energy release in propellants and fuel combustion [23,24]. It is abundant in the atmosphere. Up to now, the interaction between the HArF and HNO was not studied using the theoretical method. In order to deeply understand hydrogen bond interaction between HArF and radicals and the origin of blue- and red-shifted hydrogen bonds, we investigated the hydrogen bond formations of dimers of HArF and HNO by *ab initio* calculation. And the nature of the blue- and red-shifted hydrogen bonds was proposed. The hyperconjugative effect, rehybridizative effect and electron denisty redistribution effect on the changes of IR were discussed in detail.

_____

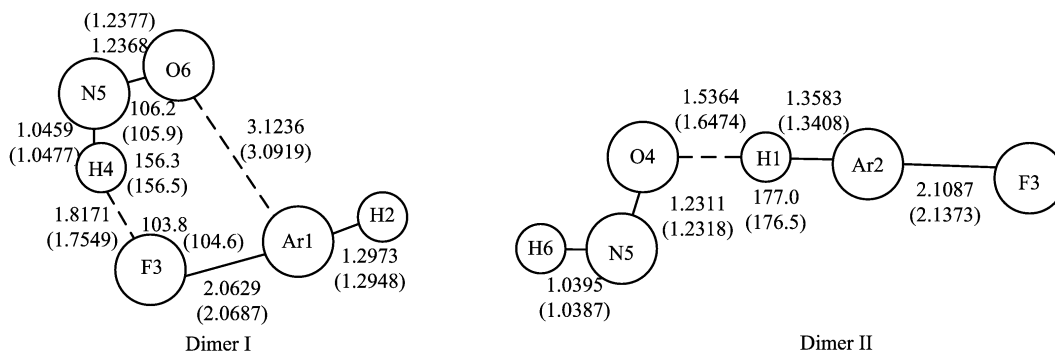*Author to whom correspondence should be addressed. E-mail: lying@aiofm.ac.cn

FIG. 1 Optimized geometries of the HNO$\cdots$HArF dimers at MP2/6-311++G(2d,2p) level with the CP corrected and uncorrected levels (in the bracket) (Bond lengths in Å, Bond angles in (°)).

II. COMPUTATIONAL METHODS

Calculations were performed using the Gaussian03 program system [25]. Both standard and counterpoise-corrected gradient optimization calculations were carried out at MP2/6-311+G**, MP2/6-311++G** and MP2/6-311++G(2d,2p) levels. And standard and counterpoise-corrected harmonic vibrational frequency calculations were performed at MP2 theory in conjunction with different basis sets to confirm whether the predicted structure is a minimum and to evaluate zero-point vibrational energies (ZPVE) corrections. The basis set superposition errors (BSSE) were calculated according to the counterpoise method proposed by Boys and Bernardi [26]. Moreover, the comparison between the DFT and MP2 vibrational calculations was performed in order to confirm the blue-shifted hydrogen bond N$-$H$\cdots$F. The G2MP2 calculations were carried out to study the interaction energies of the system. Atom in molecule (AIM) of Bader [27] was also used for topological analysis of title dimers. The charge distribution has been analyzed from the natural bond orbital (NBO) [28] partitioning scheme at the MP2/6-311++G(2d,2p) level.

III. RESULTS AND DISCUSSION

A. Geometries, frequencies and energies

Figure 1 described the optimized bond lengths, bond angles at MP2/6-311++G(2d,2p) with uncorrected and CP-corrected levels for the Dimer I (H$\cdots$F) and II(H$\cdots$O). The differences bond lengths of dimers and monomers vibrational frequencies of the N$-$H(Dimer I) and Ar$-$H(Dimer II) bonds and interaction energies at MP2 in conjunction with 6-311+G**, 6-311++G** and 6-311++G(2d,2p) basis sets with uncorrected and CP-corrected levels were listed in Table I. And the corresponding interaction energies obtained at G2MP2 levels were also listed in Table I.

Dimer I(H$\cdots$F) exhibits a five-numbered cyclic con-

formation, F3 accepting a proton from the H4, forming one hydrogen bond of N5$-$H4$\cdots$F3. Moreover, O6 interacts with Ar1 by the Coulombic electrostatic attraction. The interaction distances are 1.8171 and 3.1236 Å obtained from MP2/6-311++G (2d,2p) with CP-corrected method, 1.7549 and 3.0919 Å obtained with uncorrected method. Furthermore, the cyclic arrangement results in more bent hydrogen bond, the departure of the N5$-$H4$\cdots$F3 angle from the linearity is 23.7° (23.5°). For the Dimer II(H$\cdots$O), O4 accepts a proton from the H1 forming interaction of O4$\cdots$H1$-$Ar2. The interaction distances are 1.6474 Å obtained from MP2/6-311++G(2d,2p) with CP-corrected method and 1.5364 Å obtained with uncorrected method. The bond angle for O4$\cdots$H1$-$Ar2 is 177° (176.5°).

As far as the H-bond type prediction is concerned, taking the (HF)$_2$ complex as an example, Hobza *et al.* have pointed out the necessity of using the CP-corrected gradient optimization [29]. The CP-corrected gradient optimization will affect not only the interaction energy but also the geometry and stretching frequency of the X$-$H$\cdots$Y hydrogen bond. The uncorrected and CP-corrected calculations on the vibrational frequencies were performed at MP2 in conjunction with various basis sets. For the Dimer I(H$\cdots$F), a blue-shifted N5$-$H4$\cdots$F3 hydrogen bond is found at MP2 level. In order to confirm the blue-shifted hydrogen bond, the B3LYP calculations on vibrational frequencies were also performed and the corresponding results were listed in Table I. All calculations indicate there is a blue-shifted vibrational frequency in the Dimer I(H$\cdots$F). It is worthy of pointing out that the values of blue-shift obtained at MP2 with CP-corrected level are in agreement with those obtained at B3LYP uncorrected and CP-corrected levels. Moreover, the values of blue-shifts obtained at B3LYP with CP-corrected level are a slight larger than those obtained at B3LYP uncorrected level. However, the uncorrected MP2 calculations indicate the N$-$H elongates (+0.0009, +0.0007 and +0.0008 Å) in the Dimer I to the monomer. The corresponding vibration frequencies are blue-shifted (+8, +11 and

TABLE I Characteristics of the Dimer I and II optimization, vibrational frequencies and interaction energies at different level

	MP2/6-311+G**	MP2/6-311++G**	MP2/6-311++G(2d,2p)	G2MP2
Dimer I				
$\triangle r_{(N5-H4)standard}$/Å	+0.0009	+0.0007	+0.0008	
	(−0.0026)	(−0.0029)	(−0.0028)	
$\triangle r_{(N5-H4)cp}$/Å	−0.0019	−0.0019	−0.001	
	(−0.0032)	(−0.0033)	(−0.0032)	
$\triangle \nu_{(N5-H4)standard}$/cm^{-1}	+8(+57)	+11(+59)	+21(+71)	
$\triangle \nu_{(N5-H4)cp}$/cm^{-1}	+54(+64)	+56(+62)	+46(+74)	
$\triangle E_{standard}$/(kJ/mol)	−47.53(−39.29)	−47.53(−39.00)	−43.43(−34.32)	−50.95
$\triangle E_{cp}$/(kJ/mol)	−37.70(−35.86)	−35.86(−35.61)	−35.82(−31.77)	
Dimer II				
$\triangle r_{(Ar2-H2)standard}$/Å	+0.0589	+0.0605	+0.0324	
$\triangle r_{(Ar2-H2)cp}$/Å	+0.0133	+0.0129	+0.0149	
$\triangle \nu_{(Ar1-H2)standard}$/cm^{-1}	−578	−577	−365	
$\triangle \nu_{(Ar1-H2)cp}$/cm^{-1}	−188	−187	−178	
$\triangle E_{standard}$/(kJ/mol)	−35.32	−35.78	−30.68	−33.69
$\triangle E_{cp}$/(kJ/mol)	−26.08	−26.04	−24.58	

There results obtained at B3LYP in conjunction with the corresponding basis sets in the brackets.
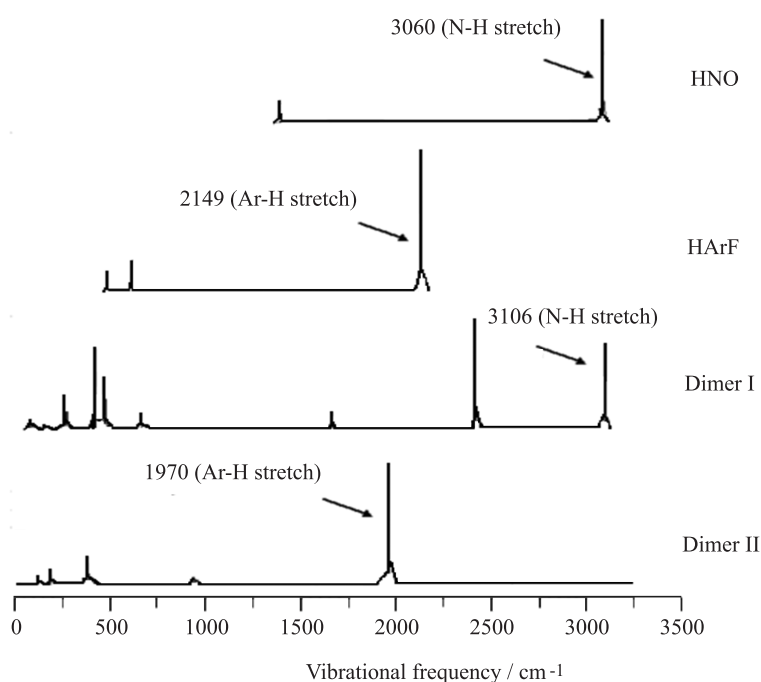

FIG. 2 Calculated IR spectra of monomers and dimers at the MP2/6-311++G(2d,2p) level.

+21 cm^{-1}). Li has attributed this abnormality of bond length change to "computational error or uncertainty" [30]. The X−H bond length change is not necessarily in accord with the vibrational frequency change. From above calculations, the N5−H4···F3 is concerned as a blue-shifted hydrogen bond. Figure 2 described the calculated IR spectra of the dimers and monomers at

MP2/6-311++G(2d,2p) level with CP corrected calculation. The MP2 with uncorrected and CP-corrected calculations show there is a red shift for the Ar−H vibrational frequencies. The values of red shifts obtained at uncorrected level are much lager than those obtained at CP-corrected level.

On the basis of these analysis, we can confirm that

TABLE II Topological parameters of the bond critical point and ring critical point at the MP2/6-311++G (2d,2p) with the CP corrected level

		Bonds	ρ	$\nabla^2\rho$	λ_1	λ_2	λ_3
BCP	Dimer I	F3$\cdots$H4	0.030189	0.1146	-0.04371	-0.04258	0.2009
		Ar1$\cdots$O6	0.0079088	0.03423	-0.007499	-0.006821	0.04855
	Dimer II	O4$\cdots$H1	0.050075	0.1067	-0.09449	-0.09174	0.2929
RCP	Dimer I	Ar1$-$F3$-$H4$-$N5$-$O6	0.005598	0.031501	-0.004489	0.00839	0.0276

the Dimer I(H$\cdots$F) possesses one blue-shifted H-bond: N$-$H$\cdots$F and there is a red-shifted vibrational frequency for Ar$-$H$\cdots$O in the Dimer II(H$\cdots$O).

As shown in Table I, the intermolecular interaction energies with both BSSE correction and ZPVE correction are in considerable agreement at various levels. The interaction energies of Dimer I(H$\cdots$F) obtained at B3LYP levels are a little lower than those obtained at MP2 and G2MP2 levels. The change trend of interaction energies from the B3LYP/6-311+G** to B3LYP/6-311++G(2d,2p) is consistent with that from the MP2/6-311+G** to MP2/6-311++G(2d,2p). Dimer II(H$\cdots$O) is less stable than Dimer I(H$\cdots$F) obtained at various methods and basis sets. And the interaction energies obtained at MP2 level are less than corresponding results obtained at G2MP2 level.

B. AIM analysis

The rigorous AIM theory has been successfully applied in characterizing hydrogen bonds of different strengths in a wide variety of molecular complexes [31,32]. Popelier proposed a set of criteria for the existence of H bonding within the AIM formalism [33]. The most prominent evidence of hydrogen bonding is the existence of a bond path between the donor hydrogen nucleus and the acceptor, containing a bond critical point (BCP) at which the electron density (ρ) ranges from 0.002 to 0.035 a.u. and the Laplacian of the electron density ($\nabla^2\rho$) ranges from 0.024 to 0.139 a.u.. According to the topological analysis of electron density in the theory of AIM, ρ is used to describe the strength of a bond. The electron density ($\nabla^2\rho$) is used to characterize the bond. Where $\nabla^2\rho<0$, the bond is covalent bond, as $\nabla^2\rho>0$, the bond belongs to the ionic bond, hydrogen bond and van der Waals interaction. Here, $\nabla^2\rho=\lambda_1+\lambda_2+\lambda_3$, λ_i is an eigenvalue of the Hessian matrix of ρ. Then, when one of the three λ_i is positive and the other two are negative, we denote it by $(3,-1)$ and call it the bond critical point (BCP). When one of the three λ_i is negative and the other two are positive, we denote it by $(3,+1)$ and call it the ring critical point (RCP), which indicates that a ring structure exists. As shown in Table II, for the Dimer I(H$\cdots$F), it is a five-membered structure by AIM. A RCP(Ar1$-$F3$-$H4$-$N5$-$O6) appeared. The value of the electron density ρ for F3$\cdots$H4 in the Dimer

I(H$\cdots$F) is 0.030189 a.u., and the value of the $\nabla^2\rho$ for F3$\cdots$H4 is 0.1146 a.u.. These values fall within the proposed typical range of the H-bonds. In addition, the Coulombic electrostatic attraction exists between the positive Ar1 atom of HArF and the negative O6 atom of HNO. For the Dimer II(H$\cdots$O), the values of the electron density ρ for O4$\cdots$H1 in the Dimer II(H$\cdots$O) is 0.050075 a.u., the value of the $\nabla^2\rho$ for O4$\cdots$H1 is 0.1067 a.u.. The value of the electron density ρ for O4$\cdots$H1 is beyond the usual value (0.04 a.u.). McDowell investigated the electron density ρ(F$\cdots$H) of HF$\cdots$HArF complex, which is more than 0.04 a.u. and proposed that the interaction of HF$\cdots$HArF complex is attributed to ionic interaction instead of the hydrogen bond interaction. For Dimer II(H$\cdots$O), it will be discussed in the NBO analysis section whether the ionic interaction or the hydrogen bond interaction plays a dominant role. The bond strength of Dimer I(H$\cdots$F) is weaker than that of the Dimer II(H$\cdots$O). However, the hydrogen bond and Coulombic electrostatic attraction together make the Dimer I(H$\cdots$F) more stable than the Dimer II(H$\cdots$O).

It should be pointed out that the N5$-$H4 bond exhibits a blue shift. However, the AIM analysis does not reveal the origin of the blue-shifted H-bond. This problem was solved by performing the natural bond orbital (NBO) analysis.

C. NBO analysis

Dimer I(H$\cdots$F) possesses one blue-shifted H-bonds, N5$-$H4$\cdots$F3. Dimer II(H$\cdots$O) exhibits one red-shifted Ar2$-$H1 vibrational frequency. To interpret the origins of the red-shifted and blue-shifted H-bonds in the Dimer I(H$\cdots$F) and II(H$\cdots$O), we performed the NBO analysis and the corresponding results are presented in Table III. In the NBO analysis, the importance of hyperconjugation interaction and electron density transfer (EDT) from lone electron pairs of the Y atom to the X$-$H antibonding orbital in the X$-$H$\cdots$Y system was well-documented [27]. In general, such interaction leads to an increase in population of X$-$H antibonding orbital. The increase of electron density in X$-$H antibonding orbital weakens the X$-$H bond, which leads to its concomitant blue shift of the X$-$H stretching frequency. Furthermore, Alabugin *et al.* have recently shown that structural reorganiza-

TABLE III NBO analysis of the HNO, HArF and Dimer I and II at the MP2/6-311++G(2d,2p) with CP-corrected level

	HNO	HArF	Dimer I	Dimer II
$E^{(2)}$ n_1(O6) $\to\sigma$ (N5−H4)/(kJ/mol)	73.48		44.98	
$E^{(2)}$ n_1(F3) $\to\sigma$ (N5−H4)/(kJ/mol)			56.76	
$E^{(2)}$ n_2(F3) $\to\sigma$ (N5−H4)/(kJ/mol)			1.71	
$E^{(2)}$ n_3(F3) $\to\sigma$ (N5−H4)/(kJ/mol)			0.46	
$E^{(2)}$ n_4(F3) $\to\sigma$ (N5−H4)/(kJ/mol)			0.29	
$E^{(2)}$ σ(N5−H6) $\to\sigma$ (Ar2−H1)/(kJ/mol)				1.09
$E^{(2)}$ σ(O4−N5) $\to\sigma$ (Ar2−H1)/(kJ/mol)				1.05
$E^{(2)}$ n_1(F3) $\to\sigma$ (Ar2−H1)/(kJ/mol)		38.84		82.05
$E^{(2)}$ n_2(F3) $\to\sigma$ (Ar2−H1)/(kJ/mol)		3.30		6.14
$E^{(2)}$ n_1(O4) $\to\sigma$ (Ar2−H1)/(kJ/mol)				177.70
$E^{(2)}$ n_2(O4) $\to\sigma$ (Ar2−H1)/(kJ/mol)				14.13
$E^{(2)}$ n_3(O4) $\to\sigma$ (Ar2−H1)/(kJ/mol)				2.01
$\triangle\sigma$ (N5−H4)/e			+0.03206	
$\triangle\sigma$ (Ar2−H1)/e				+0.05860
spn(N5−H4)	sp16.64		sp13.21	
%s-char(N in N5−H4)	83.56		99.99	
spn(Ar2−H1)		sp64.87		sp34.61
% s-char(Ar in Ar2−H1)		24.87		44.43

tion of X−H bond in the process of both blue-shifted and red-shifted H-bonds was determined by the balance of the opposing effects: X−H bond red-shifted effect due to hyperconjugative $n(Y)\to\sigma^*$(X−H) interaction and X−H bond blue-shifted effect due to rehybridization [34]. And Alabugin *et al.* predicted the value of $E^{(2)}n(Y)\to\sigma^*$(X−H) is less than 12.54 kJ/mol, then the vibrational frequencies are possible to blue shifts. However, we found the $E^{(2)}n$(F3)$\to\sigma^*$(N5−H4) is 56.76 kJ/mol and the N5−H4 blue-shifted hydrogen bond is confirmed at MP2 and B3LYP in conjunction with 6-311+G**, 6-311++G** and 6-311++G(2d,2p) basis sets. Hobza proposed that electron density redistribution was also related to the X−H contractions [35,36]. Then, we will discussion the electron density redistribution effect on the red- and blue-shifted hydrogen bonds in detail. In the type Z−X−H···Y H-bond, where Z is an electronegative atom having one or more lone electron pairs (such as F, O, N), the hyperconjugative $n(Y)\to\sigma^*$(X−H) interaction leads to an increase of electron density in the σ^*(X−H). On the other hand, a decrease in the $n(Z)\to\sigma^*$(X−H) interaction of the dimer relative to the monomer, has the opposite effect. As a result, the net change of electron density in the σ^*(X−H) and the ultimate direction of the X−H bond length change depend on the balance of these two interactions which changed in an antiparallel way. When the hyperconjugative effect inhibited electron density redistribution effect, the electron density in the σ^*(X−H) increased. When the hyperconjugative effect was inhibited by electron density redistribution effect, the electron density in the σ^*(X−H) decreased. On the basis of the theoretical model, we discussed about

the hyperconjugative effects on the blue or red shift hydrogen bonds. From Table III, the differences between the dimers and monomers for the electron density in the σ^*(N5−H4) and σ^*(Ar2−H1) are +0.00767 and +0.01402 e respectively, which indicates the hyperconjugative effect inhibites electron density redistribution effect. For the rehybridizative effect, the s-character of N5 in the N5−H4 in the Dimer I(H···F) and that of Ar2 of Ar2−H1 in the Dimer II(H···O) are more than those of the monomers from the Table III. The rehybridizative effect makes the N5−H4 and Ar2−H1 bonds blue-shifted. The competition formed between the two blue-shifted effects, rehybridizative effect and electron density redistribution effect and the red-shifted effect, hyperconjugative effect. Consequently, the cooperative effects of rehybridization and electron density redistribution inhibit the hyperconjugative effect, which leads to the N5−H4 blue shift. For the Ar2−H1 bond, the hyperconjugative effect overshadows the rehybridzative effect and electron density redistribution effect, which leads to the Ar2−H1 red shift.

Moreover, which one between the ionic interaction and the hydrogen bond interaction played a dominant role for the interaction in the Dimer II(H···O)? From Table III, the values of $E^{(2)}n$(O4)$\to\sigma^*$(Ar2−H1) are 177.70, 14.13 and 2.01 kJ/mol, that is to say, the interaction is attributed to the lone pair O atom (the proton acceptor) interacting with the σ^*(Ar2−H1) (the proton donor). All indicate that the interaction is due to the hydrogen bond interaction [37].

In summary, the hyperconjugative effect usually elongates the X−H, which leads to the H-bonds red shift. In the opposite direction, the electron density redis-

tribution effect and rehybridizative effect contract the X−H, which lead to the H-bonds blue shifts. The hydrogen bond shift is attributed to the balance between the hyperconjugative effect and electron density redistribution, rehybridizative effects.

IV. CONCLUSION

The hydrogen bonding interaction of 1:1 dimer formed between HNO and HArF molecule has been analyzed by *ab initio* method employing different basis sets. Both standard and CP-corrected calculations were performed for the structure optimizations, vibrational frequencies and interaction energies. Two stable structures are considered. BSSE corrected and G2MP2 level calculations show that the five-membered hydrogen bond Dimer I(H$\cdots$F) is more stable than Dimer II(H$\cdots$O). From the vibrational frequencies calculations, Dimer I(H$\cdots$F) exhibits one blue-shifted hydrogen bond N−H$\cdots$F. For the Dimer II(H$\cdots$O), there is a red-shifted hydrogen bond Ar−H$\cdots$O. The origin of the red- and blue-shifted hydrogen bonds was proposed from the NBO analysis. Hyperconjugative effect, rehybridizative effect and electron density redistribution effect were discussed in detail. For the blue-shifted hydrogen bond, rehybridzative and electron density redistribution effects play a dominant role. For the red-shifted hydrogen bond, hyperconjugative effect overshadows the other two effects.

V. ACKNOWLEDGMENT

[1] L. Khriachtchev, M. Pettersson, N. Runeberg, J. Lundell and M. Räsänen, Nature **406**, 874 (2000).
[2] M. Pettersson, J. Lundell and M. Räsänen, J. Chem. Phys. **102**, 6423 (1995).
[3] M. Pettersson, J. Lundell and M. Räsänen, J. Chem. Phys. **103**, 205 (1995).
[4] L. Khriachtchev, M. Pettersson, J. Lundell and M. Räsänen, J. Am. Chem. Soc. **123**, 8610 (2001).
[5] M. Pettersson, L. Khriachtchev, J. Lundell and M. Räsänen, J. Chem. Phys. **116**, 2508 (2002).
[6] A. V. Nemukhin, B. L. Grigorenko, L. Khriachtchev, H. Tanskanen and M. Pettersson, J. Am. Chem. Soc. **124**, 10706 (2002).
[7] L. Khriachtchev, Tanskanen H, Lundell J, Pettersson M, Kiljunen H and M. Räsänen, J. Am. Chem. Soc. **125**, 4696 (2003).
[8] V. I. Feldman, F. F. Sukhov, A. Y. Orlov and I. V. Tyulpina, J. Am. Chem. Soc. **125**, 4698 (2003).
[9] L. Khriachtchev, H. Tanskanen, A. Cohen, R. B. Gerber, J. Lundell, M. Pettersson, H. Kiljunen and M. Räsänen, J. Am. Chem. Soc. **125**, 6876 (2003).
[10] S. Seidel and K. Seppelt, Science **290**, 117 (2000).
[11] T. Drews, S. Seidel and K. Seppelt, Angew. Chem. Int. Ed. **41**, 454 (2002).
[12] J. Li, B. E. Bursten, B. Liang and L. Andrews, Science **295**, 2242 (2002).
[13] L. Andrews, B. Liang, J. Li and B. E. Bursten J. Am. Chem. Soc. **125**, 3126 (2003).
[14] K. O. Christe, Angew. Chem. Int. Ed. **40**, 1419 (2002).
[15] N. Runeberg, M. Pettersson, L. Khriachtchev, J. Lundell and M. Räsänen, J. Chem. Phys. **114**, 836 (2001).
[16] M. W. Wong, J. Am. Chem. Soc. **122**, 6289 (2002).
[17] J. Lundell, G. M. Chaban and R. B. Gerber, Chem. Phys. Lett. **331**, 308 (2000).
[18] A. Lignell, L. Khriachtchev, M. Pettersson and M. Räsänen, J. Chem. Phys. **117**, 961 (2002).
[19] A. Lignell, L. Khriachtchev, M. Pettersson and M. Räsänen, J. Chem. Phys. **118**, 11120 (2003).
[20] S. A. C. McDowell, J. Chem. Phys. **118**, 7283 (2003).
[21] S. A. C. McDowell, Phys. Chem. Chem. Phys. **5**, 808 (2003).
[22] S. A. C. McDowell, Chem. Phys. Lett. **368**, 649 (2003).
[23] L. C. Li, H. P. Zhou and Z. H. Tang, Chin. J. Chem. Phys. **14**, 47 (2001).
[24] A. F. Jalbout, A. M. Darwish and H. Y. Alkahby, J. Mol. Struct. (Theochem) **585**, 199 (2001).
[25] M. J. Frisch, G. W. Trucks, H. B. Schlegel, *et al. Gaussian 03 revision A.6*, Pittsburgh, PA: Gaussian, Inc., (2003).
[26] S. F. Boys and F. Bernardi, Mol. Phys. **100**, 65 (1970).
[27] A. E. Reed, L. A. Curtiss and F. Weinhold, Chem. Rev. **88**, 899 (1988).
[28] R. F. W. Bader, *Atoms in Molecules: A Quantum Theory*, Oxford: Oxford University Press, (1990).
[29] P. Hobza and Z. Halvas Theor. Chem. Acc. **99**, 372 (1998).
[30] P. Lu, G. Q. Liu and J. C. Li, J. Mol. Struct. (Theochem.) **95**, 723 (2005).
[31] U. Koch and P. L. A. Popelier, J. Phys. Chem. **99**, 9747 (1995).
[32] P. L. A. Popelier, J. Phys. Chem. A **102**, 1873 (1998).
[33] P. Lipkowski, S. J. Grabowski, T. L. Robinson and J. Leszczynski, J. Phys. Chem. A **108**, 10865 (2004).
[34] I. V. Alabugin, M. Manoharan, S. Peabody and F. Weinhold, J. Am. Chem. Soc. **125**, 5973 (2003).
[35] J. Chocholoušová, V. Špirko and P. Hobza, Phys. Chem. Chem. Phys. **6**, 37 (2004).
[36] P. Hobza and V. Ǎpirko, Phys. Chem. Chem. Phys. **5**, 1290 (2003).
[37] P. Hobza and Z. Halvas, Chem. Rev. **100**, 4253 (2000).